Jump-Diffusion Processes: Volatility Smile Fitting and Numerical Methods for Option Pricing

LEIF ANDERSEN*   landerse@genre.com
Gen Re Securities

JESPER ANDREASEN**
Bank of America

Abstract. This paper discusses extensions of the implied diffusion approach of Dupire (1994) to asset processes with Poisson jumps. We show that this extension yields important model improvements, particularly in the dynamics of the implied volatility surface. The paper derives a forward PIDE (Partial Integro-Differential Equation) and demonstrates how this equation can be used to fit the model to European option prices. For numerical pricing of general contingent claims, we develop an ADI finite difference method that is shown to be unconditionally stable and, if combined with Fast Fourier Transform methods, computationally efficient. The paper contains several detailed examples from the S&P500 market.

Keywords: jump-diffusion process, local time, forward equation, volatility smile, ADI finite difference method, fast Fourier transform

JEL classification: G13, C14, C63, D52

The standard Black-Scholes (1973) assumption of log-normal stock diffusion with constant volatility is, as all market participants are keenly aware of, flawed. To equate the Black-Scholes formula with quoted prices of European calls and puts, it is thus generally necessary to use different volatilities (so-called *implied volatilities*) for different option strikes (K) and maturities (T). The phenomenon is often referred to as the volatility *skew* or *smile* (depending on the shape of the mapping of implied volatility as a function of K and T) and exists in all major stock index markets today. Before the crash of 1987, the S&P500 volatilities, for instance, formed a "smile" pattern, where deeply in- or out-of-the-money options were characterized by higher volatilities than at-the-money options. The post-crash shape of S&P500 implied volatilities, on the other hand, more resembles a "skew" or "sneer", where implied volatilities decrease monotonically with increasing strikes. Typically, the steepness of the skew decreases with increasing option maturities. The existence of the skew is often attributed to fear of large downward market movements (sometimes known as "crash-o-phobia").

Extensions of the Black-Scholes model that capture the existence of volatility smiles can, broadly speaking, be grouped in three approaches. In the *stochastic volatility approach*

---

*   Contact author: 630 5th Avenue, Suite 450, New York, NY 10111.
**   The work in this paper was completed while this author was employed by Gen Re Securities.

(see, for instance, Heston (1993), Stein and Stein (1991), and Hull and White (1987)), the volatility of the stock is assumed to be a mean reverting diffusion process, typically correlated with the stock process itself. Depending on the correlation and the parameters of the volatility process, a variety of volatility skews and smiles can be generated in this model. Empirical evidence from time-series analysis generally shows some evidence of stochastic volatility in stock prices (see e.g. Andersen, Benzoni, and Lund (1999) for a review and many references). However, in order to generate implied Black-Scholes volatility skews in a stochastic volatility model that are consistent with those observed in traded options, often unrealistically high negative correlation between the stock index and volatility is required. Also, from a computational perspective, stochastic volatility models are complicated to handle as they are true multi-factor models; as such, one would typically need multi-dimensional lattices to evaluate, say, American options. We notice that stochastic volatility models do not allow for perfect option hedging by dynamic positions in the stock and the money market account (which in absence of other traded contracts form an incomplete market).

Another approach, originally suggested by Merton (1976), generates volatility skews and smiles by adding discontinuous (Poisson) jumps to the Black-Scholes diffusion dynamics. Again, by choosing the parameters of the jump process appropriately, this so-called *jump-diffusion* model can generate a multitude of volatility smiles and skews. In particular, by setting the mean of the jump process to be negative, steep short-term skews (which are typical in practice) are easily captured in this framework. Indeed, several authors (e.g. Das and Foresi (1996), Bates (1996), and Bakshi, Cao, and Chen (1997)) point out the importance of a jump component when pricing options close to maturity. Like stochastic volatility models, jump-diffusion models are challenging to handle numerically (an issue we shall spend considerable time on in this paper) and result in stocks and bonds forming an incomplete market.[1] Some papers dealing with either empirical or theoretical issues related to jump-diffusion models include Ait-Sahalia, Wang, and Yared (1998), Andersen, Benzoni, and Lund (1999), Ball and Torous (1985), Bates (1991), Duffie, Pan, and Singleton (1999), and Laurent and Leisen (1998).

The third approach to volatility smile modeling retains the pure one-factor diffusion framework of the Black-Scholes model, but extends it by allowing the stock volatility be a deterministic function of time and the stock price. This so-called *deterministic volatility function* (DVF) approach was pioneered by Dupire (1994), Derman and Kani (1994), and Rubinstein (1994), and has subsequently been extended or improved by many authors, including Andersen and Brotherton-Ratcliffe (1998), Andreasen (1997), Lagnado and Osher (1997), Brown and Toft (1999), Jackwerth (1996), Chriss (1996), and many others. The DVF approach has enjoyed a certain popularity with practitioners, at least partly because of its simplicity and the fact that it conveniently retains the market completeness of the Black-Scholes model. Moreover, the existence of a *forward equation* that describes the evolution of call option prices as functions of maturity and strike makes it possible to express the unknown volatility function directly in terms of known option prices. This again allows for efficient non-parametric fitting of the volatility function and, in principle at least, a precise fit to quoted market prices. In contrast, stochastic volatility models and jump-diffusion models are normally parameterized in a few param-

eters and consequently subject to fitting errors that often are unacceptably large. While convenient, the DVF model suffers from several serious drawbacks. For one, the mechanism by which the volatility smile is incorporated is clearly not realistic—few market participants would seriously attribute the existence of the volatility smile solely to time- and stock-dependent volatility. Indeed, there is much empirical literature rejecting DVF models and their implications for hedging and market completeness (e.g. Ait-Sahalia, Wang, and Yared (1998), Andersen, Benzoni, and Lund al (1999), Buraschi and Jackwerth (1998), and Dumas, Fleming, and Whaley (1997)). The weak empirical evidence is not surprising, as the DVF framework typically results in strongly non-stationary implied volatilities, often predicting that the skew of implied volatilities will vanish in the near future (see Section 4.1 for an example). In practice, however, volatility skews appear quite stationary through time. Moreover, to fit DVF models to the often quite steep short-term skew, the fitted implied volatility function must be contorted in quite dramatic, and not very convincing, fashion. This has implications not only for the pricing of exotics options, but also affects the hedge parameters for standard European options.

As discussed in Andersen, Benzoni, and Lund (1999), Bates (1996), and Bakshi, Cao, and Chen (1997), the most reasonable model of stock prices would likely include *both* stochastic volatility and jump diffusion as in the models by Bates (1996) and Duffie, Pan, and Singleton (1999). From the perspective of the financial engineer, such a model would, however, not necessarily be very attractive as it would be difficult to handle numerically and slow to calibrate accurately to quoted prices. Rather than working with such a "complete" model, this paper more modestly assumes that stock dynamics can be described by a jump diffusion process where the diffusion volatility is of the DVF-type. As we will show, this combines the best of the two approaches: ease of modeling steep short-term volatility skews (jumps) and accurate fitting to quoted option prices (DVF diffusion). In particular, by letting the jump-part of the process dynamics explain a significant part of the volatility smile/skew, we generally obtain a "reasonable", stable DVF function, without the extreme short-term variation typical of the pure diffusion approach.

The rest of this paper is organized as follows. In Section 1 we outline our process assumptions and develop a general forward PIDE describing the evolution of European call options as functions of strike and maturity. Paying special attention to the case of log-normal jumps, this section also discusses the applications of the forward PIDE to the problem of fitting the stock process to observable option prices. Section 2 illustrates the proposed techniques by applying them to the S&P500 market. The section also discusses certain hedging issues, and contains a brief general equilibrium analysis that provides a link between the risk-neutral and objective probability measures, allowing us to sanity-check our estimated risk-neutral S&P500 process parameters. In Section 3 we turn to the development of efficient finite difference methods that allow for general option pricing under the jump-diffusion processes used in this paper. We also discuss the application of Monte Carlo methods. The pricing algorithms are tested in Section 4 on both European and exotic options. Section 4 also attempts to quantify the impact of stock price jumps on certain exotic option contracts. Finally, Section 5 contains the conclusions of the paper.

1. Forward Equations for European Call Options

1.1. General Framework

Consider a stock S affected by two sources of uncertainty: a standard one-dimensional Brownian motion $W(t)$, and a Poisson counting process $\pi(t)$ with deterministic jump intensity $\lambda(t)$. Specifically, we will assume that the risk-neutral evolution[2] of S is given by[3]:

$$dS(t)/S(t-) = (r(t) - q(t) - \lambda(t)m(t)) \, dt + \sigma(t, S(t-)) \, dW(t)$$
$$+ (J(t) - 1) \, d\pi(t). \tag{1}$$

where $\{J(t)\}_{t \geq 0}$ is a sequence of positive, independent stochastic variables with, at most, time-dependent density $\zeta(\cdot; t)$. Also in (1), σ is a bounded time- and state-dependent local volatility function; m is a deterministic function given by $m(t) \equiv E[J(t) - 1]$; and r and q are the deterministic risk-free interest rate and dividend yield, respectively. We assume that π, W, and J are all independent. In (1), $t-$ is the usual notation for the limit $t - |\varepsilon|, \varepsilon \to 0$.

Under (1), the stock price dynamics consist of geometric Brownian motion with state-dependent volatility, overlaid with random jumps of random magnitude $S(J - 1)$. Notice that when the jump probability λ approaches 0, (1) becomes identical to the diffusion dynamics assumed in most previous work on volatility smiles (e.g. Dupire (1994), Rubinstein (1994), Derman and Kani (1994), Andersen and Brotherton-Ratcliffe (1998), and Andreasen (1997)).

Using standard arguments (see e.g. Merton (1976)), it is easy to show that any European-style contingent claim written on S will have a price $F = F(t, S(t))$ that satisfies the *backward partial integro-differential equation (PIDE)*

$$F_t + (r(t) - q(t) - \lambda(t)m(t))SF_S + \tfrac{1}{2}J^2(t, S)S^2 F_{SS} + \lambda(t)E[\Delta F] = r(t)F, \tag{2}$$

$$E[\Delta F(t, S)] = E[F(t, J(t)S)] - F(t, S) = \int_0^\infty F(t, Sz)\zeta(z; t) \, dz - F(t, S), \tag{3}$$

subject to appropriate boundary conditions for $F(T, S)$. In (2), subscripts are used to denote partial differentiation (so F_t equals $\partial F/\partial t$, and so on).

In (2), r and q can be deduced from quoted stock forwards and bond prices. We wish to derive the remaining terms in (2) from prices $C(t, S; T, K)$ of European call options,[4] spanning all maturities T and strikes K. To this end, consider the following proposition:

Proposition 1 *When S evolves according to (1), a European call option $C(t, S; T, K)$ satisfies the forward PIDE equation*

$$-C_T + (q(T) - r(T) + \lambda(T)m(T))KC_K + \tfrac{1}{2}\sigma(T, K)^2 K^2 C_{KK}$$
$$+ \lambda'(T)E'[\Delta'C] = q(T)C \tag{4}$$

subject to $C(t, S(t); t, K) = (S(t) - K)^+$. In (4), $\lambda'(T) = (1 + m(T))\lambda(T)$, and

$$E'\left[\Delta'C(t, S; T, K)\right] = (1 + m(T))^{-1} E\left[J(T)C(t, S; T, K/J(T))\right] - C(t.S; T, K)$$

$$= \int_0^\infty C(t, S; T, K/z)\zeta'(z; T)\,dz - C(t, S; T, K) \tag{5}$$

where ζ' is a Radon-Nikodym transformed density given by $\zeta'(z; T) = \frac{z}{1+m(T)}\zeta(z; T)$.

Proof. The proof is based on an application of the Tanaka-Meyer extension of Ito's lemma. See Appendix for details.

While not necessary for our purposes, we point out that it is also possible to extend (4) to the case where volatility is stochastic.[5] While our proof of (4) uses the Tanaka formula, independent work of Pappalardo (1996) demonstrates that the forward equation can also be constructed by integrating a jump-adjusted Fokker-Planck equation.[6]

In its most general form, equation (4) contains too many degrees of freedom to allow for a unique process (1) consistent with quoted call option prices. For practical applications, it is thus necessary to restrict, through parameterization, some of the terms in (4). For instance, we could parameterize the local volatility function (σ) directly and attempt to construct the jump density ζ by solving the resulting series of inhomogeneous integral equations. As the resulting equations belong to the class of Fredholm equations of the first kind, their solution is, however, quite involved and would likely require regularization and use of a priori information (see e.g. Press *et al.* (1992), Chapter 18). Instead, we prefer to parameterize the jump process and imply (non-parametrically) the local volatility function σ. We will discuss this technique in the following section.

1.2. *The Case of State-Dependent Local Volatility and Log-Normal Jumps*

As in Merton (1976), we now assume that the jump intensity λ is constant and that $\ln J$ is normally distributed with constant mean μ and variance γ^2, such that $E[J(t)] = \exp\left(\mu + \frac{1}{2}\gamma^2\right)$. We will assume that the constant parameters μ, γ, λ are all known, either from a historical analysis, or, as discussed further in Section 2, from a best-fit procedure applied to quoted option prices. To conveniently remove the dependence on r and q, introduce $x(u) = S(u)/F(t, u)$, $u > t$, where $F(t, u) = S(t) \exp \int_t^u [r(\tau) - q(\tau)]\,d\tau$ is the time t forward price of S delivered at time u. We note that, by standard theory,

$$\frac{C(t, S(t); T, K)}{F(t, T)} e^{\int_t^T r(s)\,ds} = E_t\left[(x(T) - k)^+\right] \equiv \Psi(t; T, k), \quad k \equiv K/F(t, T). \tag{6}$$

From Proposition 1, (6) and the assumption of log-normal jumps gives the forward PIDE

$$-\Psi_T + (\lambda' - \lambda)k\Psi_k + \frac{1}{2}s(T, k)^2 k^2 \Psi_{kk}$$

$$+ \lambda'\left(\int_{-\infty}^\infty \Psi(t; T, ke^{-\mu-\gamma z})\varphi(z - \gamma)\,dz - \Psi\right) = 0. \tag{7}$$

where $\lambda' = \lambda e^{\mu + \frac{1}{2}\gamma^2}$, φ is a standard Gaussian density, and $s(u, x(u)) \equiv \sigma(u, S(u))$. It is clear that if we know the function $C(t, S; T, K)$ and its derivatives for all T and K, then

we can construct the local volatility function σ directly from (6)–(7).[7] In reality, however, only a limited set of call prices $C(t, S; T, K)$ is quoted in the market, making the inverse problem ill-posed. A variety of regularization techniques can be applied to overcome this problem, the simplest of which involves sufficiently smooth interpolation and extrapolation of known data (see e.g. Andersen and Brotherton-Ratcliffe (1998), and Andreasen (1997)). This technique, which effectively extends the input price set to cover all values of K and T, will also be employed in this paper.[8] An alternative approach assumes a specific form of the local volatility function (e.g. a spline as in Coleman, Li, and Verma (1999)) and finds an optimal[9] fit to quoted option prices by large-scale iterative methods. The existence of a forward equation (4) significantly improves the speed of such methods, as option prices with different strikes and maturities can be priced in a single finite difference grid.[10] Other iterative approaches along these lines can be found, for example, in Lagnado and Osher (1997) and Avallaneda *et al.* (1996). As a general comment, we point out that iterative methods that are feasible in a pure diffusion setting may become prohibitively slow for jump-diffusions due to the presence of integrals in the forward and backward equations. To improve speed, one can imagine replacing the non-parametric specification of the local volatility function with a parametric form and combining this with "bootstrapping" of the forward equation; we will briefly discuss such a technique in Section 1.3.

To proceed, we first wish to transform (7) into an equation involving implied volatilities rather than call prices. The former is normally much "flatter" as a function of K and T than the latter and significantly simplifies interpolation and extrapolation procedures. For the special case of $s(u, x(u)) = \hat{s}$ where $\hat{s}$ is a constant, we know from Merton (1976) that[11]

$$\Psi(t, T, k) = M(t; T, k, \hat{s}) \equiv \sum_{n=0}^{\infty} A(n)\Phi(d_n) - k \sum_{n=0}^{\infty} B(n)\Phi(d_n - v_n), \qquad (8)$$

$$A(n) = \frac{e^{-\lambda'(T-t)}[\lambda'(T-t)]^n}{n!}; \quad B(n) = \frac{e^{-\lambda(T-t)}[\lambda(T-t)]^n}{n!};$$

$$v_n = \sqrt{\hat{s}^2(T-t) + n\gamma^2}; \quad d_n = \frac{-\ln k + (\lambda - \lambda')(T-t) + n(\mu + \frac{1}{2}\gamma^2)}{v_n} + \frac{1}{2}v_n.$$

In (8), Φ denotes the standard cumulative normal distribution function. If $s(u, x(u))$ is not constant, we can use (6) to define an *implied Merton volatility* $\hat{s}(T, k)$ (not to be mistaken for the usual Black-Scholes implied volatility) through the equation

$$M(t, T, k, \hat{s}(T, k)) = \Psi(t; T, k), \qquad (9)$$

where the right-hand side is observed in the market.[12] Equations (7) and (9) allow us to express the local volatility $s(T, k)$ as a function of implied Merton volatility $\hat{s}(T, k)$:

Proposition 2 *Defining $k = K/F(t, T)$ and $\alpha_n \equiv \left(1 + \frac{n\gamma^2}{\hat{s}(T,K)^2(T-t)}\right)^{-1}$, the local volatility function $\sigma(T, K) = s(T, k)$ is given by the implied Merton volatility $\hat{s}(T, k)$ in (8)–(9) as follows:*

$$s(T, k) = \sqrt{num/den},$$

$$
\begin{aligned}
num &= \sqrt{T-t} \sum_{n=0}^{\infty} \sqrt{\alpha_n} A(n)\varphi(d_n) \left[\frac{\hat{s}}{2(T-t)} + (\lambda - \lambda')k\hat{s}_k + \hat{s}_T \right] \\
&\quad + \lambda' M\left(t, T, ke^{-\mu - \frac{1}{2}\gamma^2}, \sqrt{\hat{s}(k,T)^2 + \gamma^2/(T-t)} \right) \\
&\quad - \lambda E\left[JM(t, T, k/J, \hat{s}(T, k/J)) \right], \\
den &= \tfrac{1}{2} k^2 \sqrt{T-t} \sum_{n=0}^{\infty} A(n)\varphi(d_n)\sqrt{\alpha_n} \\
&\quad \times \left[\hat{s}_{kk} + \hat{s}_k^2 \left(\frac{1-\alpha_n}{\hat{s}} - d_n \sqrt{\alpha_n(T-t)} \right) + \frac{1}{\hat{s}} \left(\alpha_n d_n \hat{s}_k + \frac{1}{k\sqrt{T-t}} \right)^2 \right]
\end{aligned}
$$

Proof. Follows from insertion of (9) into (7) and a number of manipulations.

We notice that when $\hat{s}(T, k)$ is constant and equal to g, say, $\hat{s}(T, k) = s(T, k) = g$, Proposition 2 reduces to

$$
\lambda E[JM(t, T, k/J, g)] = \lambda' M\left(t, T, ke^{-\mu - \frac{1}{2}\gamma^2}, \sqrt{g^2 + \gamma^2/(T-t)} \right), \tag{10}
$$

a result that can be verified by direct computation and will be useful in the following. Also notice that when $\lambda \to 0$, Proposition 2 reduces to

$$
s(T, k)^2 = \frac{\hat{s}/(T-t) + 2\hat{s}_T}{k^2 \left(\hat{s}_{kk} - \hat{s}_k^2 d_0 \sqrt{T-t} + \frac{1}{\hat{s}} \left(d_0 \hat{s}_k + \frac{1}{k\sqrt{T-t}} \right)^2 \right)}
$$

which is a known expression for the jump-free case (see Andersen and Brotherton-Ratcliffe (1998), or Andreasen (1997)).

The infinite series in Proposition 2 are all well-behaved and typically require the evaluation of less than 5–6 terms before sufficient accuracy is achieved. For the result in Proposition 2 to be useful in practice, we only need efficient methods of computing the integral term

$$
\begin{aligned}
\lambda E\left[JM(t, T, k/J, \hat{s}(T, k/J)) \right] &= \lambda' \int_{-\infty}^{\infty} M\left(t, T, e^{\gamma(\omega - v)}, \hat{s}(T, e^{\gamma(\omega - v)}) \right) \varphi(v)\, dv \\
&\equiv I(T, \omega)
\end{aligned}
$$

where we have introduced a variable ω defined by $k = e^{\mu + \gamma^2 + \omega\gamma}$. As the function $M(\cdot)$ does not vanish for $\omega - v \to -\infty$, we proceed to separate out the part of the integrand that correspond to some (guessed) constant volatility g. That is, we define

$$
\xi(x; t, T) = M\left(t, T, e^{\gamma x}, \hat{s}(T, e^{\gamma x}) \right) - M\left(t, T, e^{\gamma x}, g \right)
$$

and can now write

$$
\begin{aligned}
I(T, \omega) &= \lambda' \int_{-\infty}^{\infty} M\left(t, T, e^{\gamma(\omega - v)}, g \right) \varphi(v)\, dv + \lambda' \int_{-\infty}^{\infty} \xi(\omega - v; t, T)\varphi(v)\, dv \\
&= \lambda' M\left(t, T, ke^{-\mu - \frac{1}{2}\gamma^2}, \sqrt{g^2 + \gamma^2/(T-t)} \right) \\
&\quad + \lambda' \int_{-\infty}^{\infty} \xi(\omega - v; t, T)\varphi(v)\, dv
\end{aligned} \tag{11}
$$

where we have used (10). We are now left with the problem of computing numerically

$$c(T, \omega) = \int_{-\infty}^{\infty} \xi(\omega - v; t, T)\varphi(v)\, dv$$

which can be interpreted as *convolution* $\xi * \varphi$ of the two functions ξ and φ. This suggests the introduction of discrete Fourier transform (DFT) methods. Specifically, assume that we are interested in evaluating $c(T, \omega)$ as a function of ω on an equidistant grid $\omega_i = \omega_0 + i\Delta$, $i = 0, 1, \ldots, N - 1$, where N is an even number and Δ some positive constant. We will assume that the grid is wide enough to ensure that $\xi(\omega_0; t, T)$ and $\xi(\omega_{N-1}; t, T)$ are close to zero.[13] Writing $\xi(\omega_i; t, T) = \xi_i$ and $\varphi(i\Delta) = \varphi_i$, the convolution can be approximated by

$$c(T, \omega_i) \approx \Delta \sum_{j=-N/2+1}^{N/2} \xi_{i-j}\varphi_j \tag{12}$$

where we account for negative indices by assuming that both ξ and φ are periodic with period N (a necessary assumption in DFT). The summation in (12) is, conveniently, the definition of the convolution operator in the theory of DFT. Using $\langle \cdot \rangle$ to denote discrete Fourier transforms, it is well-known that

$$\langle c \rangle_i / \Delta = \langle \xi \rangle_i \langle \varphi \rangle_i$$

where the index i runs over N different frequencies. $\langle \varphi \rangle$ can be constructed analytically (the Fourier transform of a Gaussian density is another Gaussian density), whereas $\langle \xi \rangle$ can be computed efficiently using Fast Fourier Transformation (FFT). Forming the complex product of $\langle \xi \rangle$ and $\langle \varphi \rangle$ and transforming back by inverse FFT gives us c. Notice that the algorithm above gives the values of c for all N values of ω on the grid simultaneously. If $N = 2^p$ for some integer p, FFT is of computational order $O(N \log_2 N)$. The algorithm above is thus also of order $O(N \log_2 N)$, a significant improvement over a direct implementation of (12) ($O(N^2)$ to evaluate c at all N values of ω). In general, we need to run the algorithm above for different values of T in some pre-defined grid. With M different values of T, the total effort of computing the convolution integrals becomes $O(MN \log_2 N)$.

1.3. A Parametric Bootstrapping Technique

While the approach discussed in the previous section is very fast, it relies quite heavily on inter- and extrapolation methods and on input prices being smooth and regular. To make this method work, it is generally necessary to pre-condition market quotes carefully, as will be discussed in detail in the next section. Before proceeding to this, we will briefly discuss a more robust bootstrapping that works with a discrete set of option prices. Suppose in particular that we want hit a range of option prices with the maturities:

$$0 = T_0 < T_1 < \cdots < T_N.$$

First, we choose a distribution of the jumps. As in the previous section, one could for example assume that J is log-normal with best-fitted parameters μ, λ, γ. For each interval $]T_i, T_{i+1}]$ let the local volatility be given by $\sigma(t, S) = g(S; \mathbf{a}_i)$ where g is some function defined by its parameter vector $\mathbf{a}_i$. Starting with $i = 0$ we now repeatedly solve (7) over the interval $]T_i, T_{i+1}]$ for changing values of the parameters $\mathbf{a}_i$, until an optimal fit to the observed option prices is obtained. A good choice for updating the parameter vector $\mathbf{a}_i$ is the Levenberg-Marquardt routine described in Press *et al.* (1992). Once the optimal $\mathbf{a}_i$ is found we proceed to the next time step. If we wish to find a perfect fit to the observed option prices each parameter vector $\mathbf{a}_i$ must have a dimension that is at least as high as the number of quoted option prices with maturity T_{i+1}.

One would think that the updating and the numerical solution of the PIDEs would prohibit the practical application of this algorithm, but this is not the case. Using the numerical PIDE solution algorithm that we present below we are typically able to fit to a 10×10 grid of observed option prices in about 15 seconds on a Pentium PC.

2. Fitting the Local Volatility Function: An Example From the S&P500 Market

In this section we illustrate the theory of the previous section by an example based on data from the S&P500 index. We will use the method outlined in Section 1.2 and consequently assume that jumps are log-normal with constant parameters (μ, γ, λ). In April 1999, the bid-offer implied Black-Scholes volatilities of European call options on the S&P500 index were as shown in Table 1. With a constant interest rate of $r = 5.59\%$ and a constant dividend yield of $q = 1.14\%$ the bid-offer spreads correspond to bid and offer option price spreads from mid as given in the second column of Table 1.

2.1. *Jump Parameter Fitting*

To determine the jump parameters, we first do a best fit (in a least-squares sense) of the Merton model (8) to the mid implied Black-Scholes volatilities of Table 1. The resulting best-fit parameters are

$$\sigma = 17.65\%, \quad \lambda = 8.90\%, \quad \mu = -88.98\%, \quad \gamma = 45.05\%.$$

Measured in terms of implied Black-Scholes volatilities, the total RMS error in the fit to the options is Table 2 is 0.014 with the largest difference for any option being 0.037. Interestingly, the best-fit continuous volatility σ is close to what one obtains by time- series estimation on historical S&P500 data (for instance, using the past 10 year's time-series of daily S&P500 returns we get a historical volatility of approximately 15.0%). The mean jump in return is $m = -54.54\%$. This number, and the estimated jump intensity λ, are higher than what one would expect from time-series data, and either indicate that the market currently perceives the chance of a big crash to be higher than normal or, more likely, that the jump parameters include significant elements of risk aversion ("market price of risk"). Indeed, all parameters above are estimated in the market risk-neutral measure, and, with the exception of the diffusion volatility, do not generally equal the objective ("historical")

parameters. The relationship between the risk-neutral and objective probability measures is governed by the jump-extended Girsanov Theorem (see Bjork, Kabanov, Runggaldier (1997)). Working in a general equilibrium framework, the link between the two probability measures can be characterized in terms of the utility of a representative agent. Section 2.3 contains a brief analysis along these lines, and demonstrates that the parameters estimated above are actually quite reasonable.

2.2. Local Volatility Fitting

To construct a local volatility surface that fits the input volatilities of Table 1, we first convert the bid and offer implied volatilities of Table 1 into a grid of implied Merton volatilities (as in (9)). We then generate a smooth surface of these volatilities that lies inside the bid and offer spread, and extrapolate to the unobservable corners of the volatility grid. The smoothing/extrapolation procedure used is described in detail in Andreasen (1997); it involves numerically solving an optimization problem with quadratic objective function and linear constraints. The resulting grid of Merton volatilities is given in Table 2. As expected from the relatively tight fit of the constant-volatility Merton model, the implied Merton volatilities are fairly, but not perfectly, flat.

The Merton volatilities can now be interpolated and extrapolated in (T, k) space, as discussed in Andersen and Brotherton-Ratcliffe (1998). Here we use a two-dimensional tensor-spline (Dierckx (1995)) which guarantees smoothness in both T- and k-directions, and conveniently allows for closed-form computations of the derivatives needed in the formula in Proposition 2. Figure 1 shows the resulting instantaneous local volatilities $\sigma(t, S)$. The local volatility surface is, essentially, U-shaped and quite stationary through time. For comparison, Figure 2 shows the local volatilities obtained by fitting a pure diffusion (DVF) model to the data in Table 1. Not surprisingly, Figure 2 shows that the local volatilities of the DVF model need to be steep and highly non-stationary in order to fit the S&P500 data. The impact of this non-stationarity on option prices will be examined in Section 4.

2.3. General Equilibrium Analysis

As discussed earlier, the jump parameters listed in Section 2.1 are estimated under the risk-neutral probability measure. To gauge whether the parameters are reasonable, we here briefly wish to demonstrate that our extreme-appearing parameter values are in fact not inconsistent with general equilibrium theory. Indeed, it is well-known that economic theory that moving from the objective probability measure to the risk-neutral probability measure results in higher jump intensity, lower mean jump, and unchanged continuous volatility. The latter is, of course, required for the two probability measures to be equivalent and constitutes a necessary condition for absence of arbitrage.

One can use the analysis in Naik and Lee (1990) to deduce that if the market has a representative agent that maximizes expected additive separable power utility of future

Table 1. Bid/Ask implied Black-Scholes volatilities in S&P500, April 1999.

Strike (K)

T	Bid/Offer		50	70	80	85	90	95	100	105	110	115	120	130	140	150	160	170	180	200
0.08	5	Bid					28.05	25.29	22.17	18.95	15.50									
		Ask					30.13	26.44	23.03	20.10	19.57									
0.25	6	Bid				30.57	28.30	25.95	23.55	21.28	19.23	17.57	15.64							
		Ask				31.75	29.16	26.61	24.13	21.88	23.03	19.03	19.28							
0.50	7	Bid				29.70	27.78	25.96	24.22	22.56	20.98	19.65	18.58	16.22						
		Ask				30.50	28.44	26.52	24.74	23.06	21.52	20.32	19.52	19.04						
0.75	9	Bid			30.96	29.36	27.74	26.15	24.61	23.22	22.01	21.02	20.14	18.50	16.40					
		Ask			31.82	30.08	28.36	26.69	25.11	23.70	22.51	21.56	20.78	19.63	19.22					
1.00	10	Bid			30.60	29.28	27.92	26.53	25.12	23.73	22.43	21.27	20.19	18.27	16.48	12.67				
		Ask			31.40	29.96	28.52	27.07	25.62	24.21	22.91	21.77	20.75	19.12	18.19	18.30				
1.50	11	Bid			30.01	28.93	27.81	26.67	25.53	24.38	23.30	22.37	21.50	19.99	18.68	17.46	16.09	10.74		
		Ask			30.69	29.53	28.35	27.17	25.99	24.82	23.74	22.81	21.96	20.53	19.41	18.64	18.29	18.46		
2.00	12	Bid			29.87	28.90	27.92	26.94	25.97	25.01	24.08	23.24	22.53	21.25	20.11	19.09	18.16	17.25	16.09	
		Ask			30.51	29.46	28.44	27.42	26.41	25.43	24.48	23.64	22.93	21.69	20.63	19.76	19.12	18.72	18.59	
3.00	15	Bid	34.24	31.64	30.04	29.24	28.44	27.64	26.84	26.06	25.29	24.56	23.93	22.94	22.04	21.24	20.55	19.97	19.45	18.52
		Ask	35.56	32.38	30.64	29.78	28.94	28.10	27.28	26.48	25.69	24.94	24.31	23.32	22.44	21.68	21.05	20.57	20.18	19.73
4.00	17	Bid	33.69	31.69	30.33	29.65	28.98	28.31	27.64	26.99	26.34	25.61	24.97	24.19	23.48	22.85	22.28	21.76	21.31	20.56
		Ask	34.94	32.41	30.91	30.19	29.48	28.77	28.08	27.41	26.74	25.99	25.35	24.55	23.84	23.23	22.68	22.20	21.79	21.18
5.00	20	Bid		31.60	30.50	29.93	29.38	28.83	28.29	27.75	27.21	26.66	26.14	25.24	24.55	23.98	23.47	22.99	22.55	21.82
		Ask		32.31	31.08	30.47	29.88	29.31	28.73	28.17	27.61	27.06	26.52	25.60	24.91	24.34	23.83	23.37	22.95	22.28
7.00	42	Bid	32.29	30.97	30.20	29.81	29.42	29.04	28.66	28.29	27.92	27.54	27.17	26.45	25.77	25.31	24.96	24.62	24.32	23.80
		Ask	34.32	32.19	31.22	30.77	30.32	29.88	29.46	29.05	28.64	28.24	27.85	27.09	26.39	25.91	25.54	25.20	24.90	24.40
10.0	75	Bid	31.07	30.50	30.09	29.86	29.63	29.38	29.15	28.91	28.68	28.44	28.20	27.73	27.25	26.78	26.31	25.98	25.77	25.39
		Ask	33.91	32.29	31.61	31.28	30.95	30.64	30.33	30.05	29.76	29.48	29.20	28.67	28.15	27.64	26.78	26.78	26.55	26.15

Note: Market bid and offer implied volatilities for the S&P 500 index. Strikes (K) are in percentage of initial spot and maturities (T) are measured in years. The second column reports approximate option price bid and ask spreads from mid in basis points (1/100 percent) of the spot index value. Volatilities are expressed in percent. Blank cells mean that there are no observations for that particular maturity and strike. The interest rate and dividend yield are 5.59% and 1.14%, respectively.

Table 2. Smooth implied Merton volatilities for S&P500.

Strike (K), % of Spot

T	50	70	80	85	90	95	100	105	110	115	120	130	140	150	160	170	180	200
0.08	19.69	19.44	18.29	21.72	21.73	22.11	20.72	19.05	18.20	17.61	17.65	15.75	15.76	14.84	14.31	14.59	15.76	20.27
0.25	19.37	19.04	18.41	20.76	21.50	21.54	20.55	19.18	18.29	17.69	17.48	16.03	15.73	15.04	14.60	14.82	15.83	1966
0.50	18.89	18.44	18.22	19.75	20.83	20.89	20.19	19.18	18.36	17.77	17.38	16.24	15.77	15.26	14.91	15.07	15.87	18.89
0.75	18.41	17.86	17.83	18.99	20.08	20.29	19.79	19.03	18.33	17.79	17.34	16.32	15.82	15.41	15.14	15.24	15.88	18.27
1.00	17.96	17.30	17.39	18.36	19.40	19.73	19.39	18.80	18.22	17.73	17.24	16.33	15.86	15.51	15.28	15.34	15.84	17.78
1.50	17.13	16.21	16.57	17.28	18.18	18.68	18.58	18.22	17.83	17.50	17.11	16.34	15.90	15.65	15.49	15.49	15.77	17.04
2.00	16.50	15.20	15.93	16.52	17.26	17.79	17.90	17.71	17.44	17.20	16.95	16.34	15.94	15.74	15.63	15.60	15.74	16.55
3.00	15.91	13.56	15.26	15.83	16.31	16.67	16.87	16.91	16.82	16.69	16.57	16.31	16.06	15.92	15.85	15.83	15.85	16.07
4.00	15.84	14.41	15.51	15.98	16.26	16.40	16.47	16.48	16.43	16.36	16.29	16.17	16.09	16.10	16.06	16.05	16.06	16.09
5.00	15.98	15.54	16.21	16.37	16.49	16.55	16.54	16.50	16.40	16.28	16.18	16.07	16.04	16.10	16.17	16.21	16.25	16.26
7.00	16.84	16.90	17.02	17.06	17.07	17.05	16.98	16.89	16.78	16.65	16.52	16.28	16.14	16.10	16.15	16.26	16.38	16.58
10.0	18.03	17.99	17.94	17.90	17.85	17.79	17.71	17.63	17.54	17.44	17.33	17.11	16,89	16.71	16.57	16.48	16.45	16.54

Note: Volatility numbers are in %. Maturities are in years and strikes are in percentage of initial spot. Jump parameters are $\lambda = 8.90\%$, $\mu = -88.98\%$, $\gamma = 45.05\%$. The interest rate and dividend yield are 5.59% and 1.14%, respectively.
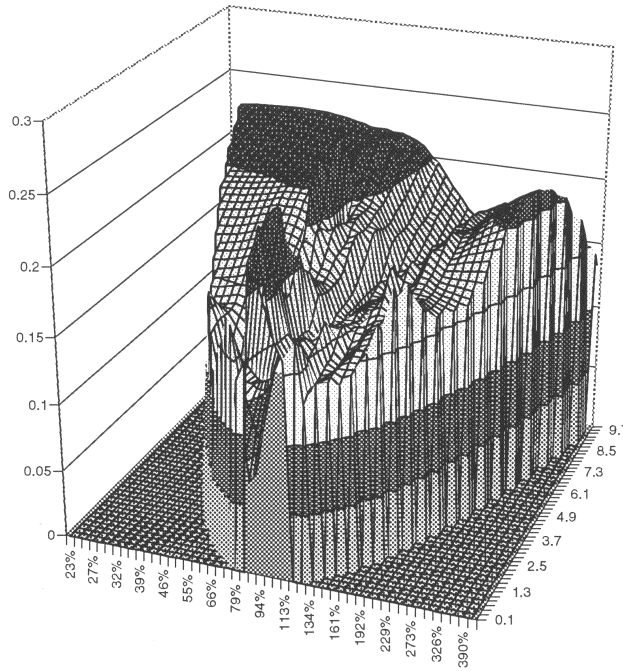
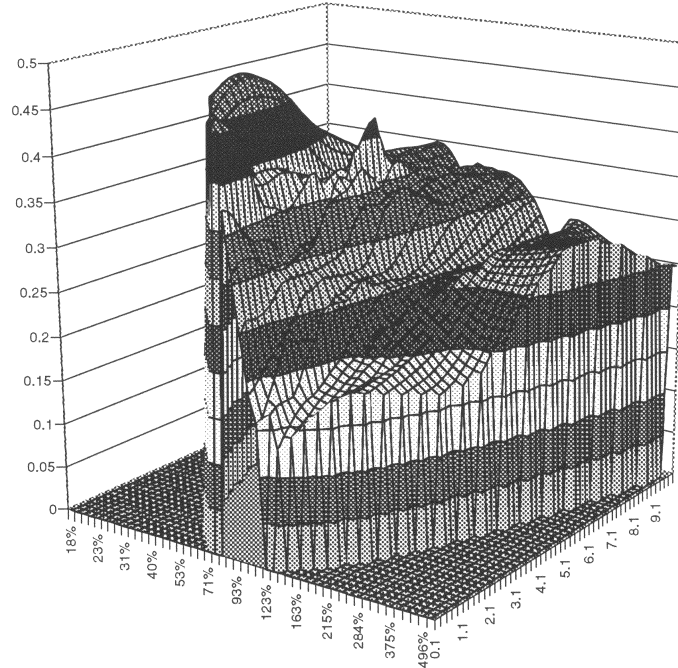*Figure 1.* Local diffusion volatilities for the S&P500 index, April 1999. Local volatilities for jump-diffusion model when fitted to S&P500 option prices. First axis is future spot relative to current spot and second axis is time in years. The local volatilities are generated on a 150×256 grid. Jump parameters are $\lambda = 8.90\%$, $\mu = -88.98\%$, $\gamma = 45.05\%$. The interest rate and dividend yield are 5.59% and 1.14%, respectively.

consumption, then the risk-neutral parameters of the jump-diffusion model are linked to the historical parameters through the relations

$$\sigma = \sigma_h, \quad \lambda = \lambda_h e^{-(1-\beta)(\mu_h + \gamma_h^2/2)}, \quad \mu = \mu_h - (1-\beta)\gamma_h^2, \quad \gamma = \gamma_h,$$

where subscript h indicates parameters under the objective measure, and $1 - \beta$ is the (constant) relative risk aversion of the representative agent. Obviously, if the representative agent is risk-averse and the mean jump is negative, then the jump intensity and the magnitude of the mean jump will both increase under the risk-neutral measure.

To use the results above in a quantitative analysis, we need estimates of the historical jump intensities and means. Unfortunately, standard empirical analysis is of little help here as the historical sample size of significant stock index jumps is extremely limited. As we are here mainly interested in a rough "sanity" check of our parameters, we instead simply note that the 20th century has experienced two large jumps in the S&P500 index (1929 and 1987) each of a magnitude of approximately -30%. If we condense this information into a historical jump intensity of about 2% and a mean jump of -30% and use our estimate of $\gamma_h = \gamma = 0.4505$ (which implies that $\mu_h = -0.4582$), then given our implied risk-neutral

Figure 2. DVF local volatilities for the S&P500 index, April 1999. Local volatilities for pure diffusion model when fitted to S&P500 option prices. First axis is future spot reative to current spot and second axis is time in years. The local volatilities are generated on a 150 × 256 grid. The interest rate and dividend yield are 5.59% and 1.14%, respectively.

jump parameters, a best-fit[14] solution for the relative risk-aversion is

$$1 - \beta^* = 3.39$$

This level of risk-aversion is by no means excessive and falls well in line with other estimates of the relative risk-aversion. This best-fit relative risk-aversion correspond to the risk-neutral jump-parameters

$$\lambda^* = 6.70\%, \quad \mu^* = -114.6\%, \quad m^* = -64.89\%.$$

These parameters are quite close to our implied risk-neutral jump parameters indicating that the "best-fit" solution is reasonable. Naik and Lee's analysis shows that the equilibrium expected excess return of the stock over the risk-free rate is given by

$$\alpha_h - r = (1 - \beta)\sigma_h^2 + (m_h\lambda_h - m\lambda)$$

Using historical parameters of $\sigma_h = 0.15$, $\lambda_h = 0.02$, $m_h = -0.30$ and our implied risk-neutral jump parameters combined with our best-fit relative risk-aversion we get an expected excess return of around 11.9%, which again is not inconsistent with empirical data.

2.4. Hedging

As discussed earlier, the jump-diffusion model implies that the stock index and the money-market account do not together form a complete market. Indeed, for most jump-diffusion processes, an infinite number of options must be traded for the market to be complete. This feature of the model is perhaps unattractive to many who are used to the easy "delta" hedges of the Black-Scholes economy. Ignoring jump risk, however, is fraught with peril as it is well-known that the Black-Scholes hedges fall apart in environments with rapid movements of the underlying assets (case in point: during the 1987 crash the "portfolio insurance" put-option delta hedges put on by many major banks failed miserably). In some sense, our jump-diffusion framework allows one to charge for such potential hedge failures in a way that is consistent with the market. That said, we shall now demonstrate that often significant parts of the jump risk can be eliminated by adding just a few option positions to a standard delta hedge. Specifically, let us consider a derivatives portfolio V marked in a Merton model with jump parameters (μ, λ). Let us assume that interest rates and stock dividends are 0 and that the historical jump parameters are (μ_h, λ_h). Using n stocks to hedge V, the evolution of the mark-to-market value of the total position satisfies (time and stock dependence suppressed for brevity)

$$d(v + nS) = \left[V_t + (\alpha_h - \lambda_h m_h) SV_s + \tfrac{1}{2}\sigma^2 S^2 V_{SS} \right] dt + V_S \sigma S dW_h + \Delta V d\pi$$
$$+ n\left[(\alpha_h - \lambda_h m_h) S dt + \sigma S dW_h + \Delta S d\pi \right]$$

where α_h is the excess stock return, W_h is a Brownian motion under the historical ("real-life") probability measure, and σ is the constant stock volatility. Setting $n = -V_S$ ("delta") and using the backward equation (2), we get

$$d(V + nS) = \lambda(mSV_s - E[\Delta V])dt + (\Delta V - V_S \Delta S)d\pi.$$

As this equation demonstrates, the delta-hedged portfolio V is not risk-free, but is exposed to jumps in the Poisson process π. To hedge away some of this risk, consider now adding ϕ call options C to the hedge. After adjusting $n = -V_S - \phi C_S$ to stay delta neutral, we get

$$d(V + nS + \phi C) = \lambda(mS(V_S + \phi C_S) - E[\Delta V + \phi \Delta C])dt +$$
$$(\Delta V + \phi \Delta C - (V_S + \phi C_s)\Delta S)d\pi.$$

ϕ can be set according to many criteria, but consider the obvious

$$\phi = -\frac{E^h[\Delta V + V_S \Delta S]}{E^h[\Delta C + C_S \Delta S]}, \tag{13}$$

where $E^h[\cdot]$ denotes expectation under the objective probability measure. With this choice, $E^h[\Delta(V + nS + \phi C)] = 0$, i.e. we have hedged away the mean portfolio jump. The hedge can be improved further by adding more options, for instance by using the standard principle of mean-variance optimization.

To test the efficiency of the hedging strategy outlined above, consider a portfolio consisting of a short position in a 2-year at-the-money call option and a long position in a 5-year at-the-money call option. Using the model parameters from Section 2.1, the figure below
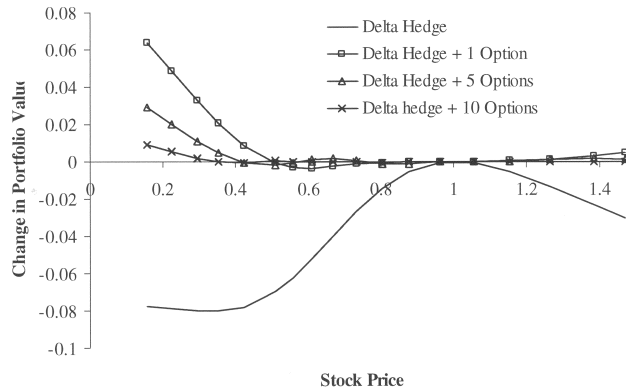
Figure 3. Performance of various hedges for sample portfolio. Performance of various hedges for portfolio consisting of a short position in a 2-year at-the-money call and a long position in a 5-year at-the-money call. *x*-axis is stock price, relative to the current price. *y*-axis is the change in portfolio value. The option hedges consist of 1-year call options, with holdings optimized to minimize variance subject to the mean jump in the total position to equal 0. Strikes used for the three option hedges in the figure are (as a percentage of current stock price): {1}, {0.9, 0.95, 1.0, 1.05, 1.1}, and {0.75, 0.8, 0.85, 0.9, 0.95, 1.0, 1.05, 1.1, 1.15, 1.2}.

shows the stock price sensitivity of the portfolio hedged a) by a delta-hedge only; and b) by a delta-hedge supplemented by various 1-year call option positions. The option positions have been found by minimizing the variance of the overall positions, subject to the mean portolio jump being 0.

As the figure shows, inclusion of just a single 1-year at-the-money call option removes significant portions of the jump risk.

3.   Numerical Methods for Option Pricing in the Jump-Diffusion Model

So far we have spent most of our efforts calibrating the jump-diffusion model to the market for European call options. For our model to be useful in practice, we need to consider numerical methods to efficiently price general contingent claims satisfying the backward PIDE (2). A related problem is the numerical solution of the forward equation (4) or (7), which would typically be required in iterative calibration methods (see discussion in Sections 1.2 and 1.3).

Very little material has been published in the finance literature on numerical methods for PIDEs of the type occurring in jump-diffusion models. A few exceptions include Amin (1993), Zhang (1993), and Andreasen and Gruenewald (1996). The methods suggested in the two first papers are essentially multinomial trees, i.e. explicit methods. Explicit methods generally suffer from instability problems as well as poor convergence in the time-domain. As is well-known from the finite difference literature, implicit methods typically exhibit better precision, convergence and stability properties than explicit methods and are preferable for option pricing problems. The paper by Andreasen and Gruenewald presents

such an implicit method that solves the pricing PIDE on a single Crank-Nicholson finite difference grid, with each time-step involving the inversion of a non-sparse matrix. In the constant-parameter setting of Andreasen and Gruenewald, the matrix inversion turns out to be computationally feasible. In our setting with time- and price-dependent volatility functions, another approach is needed. In the following subsection we describe an accurate and efficient solution technique that can be used under our model assumptions.

3.1. *The FFT-ADI Finite Difference Method*

We first notice that after appropriate logarithmic transformations the PIDEs considered so far in this paper ((2), (4), and (7)) can all be written in the form:

$$0 = \frac{\partial F}{\partial t} + \left[-r + a\frac{\partial}{\partial x} + \tfrac{1}{2}b^2\frac{\partial^2}{\partial x^2} \right] F + \lambda \int_{-\infty}^{+\infty} \varsigma(t, x-y)F(t, y)\,dy - \lambda F \quad (14)$$

where[15] $\varsigma(t, \cdot)$ is a density function, and $r = r(t)$, $a = a(t, x)$, $b = b(t, x)$, $\lambda = \lambda(t)$. Defining

$$D \equiv -r + a\frac{\partial}{\partial x} + \tfrac{1}{2}b^2\frac{\partial^2}{\partial x^2}$$

and using the convolution operator * we can write (14) in the more compact form

$$0 = \frac{\partial F}{\partial t} + DF - \lambda F + \lambda\varsigma^*F. \quad (15)$$

Interpreting $F(t) = F(t, \cdot)$ we can discretize (15) in the time-dimension as follows:

$$\begin{aligned} 0 \;=\; & \Delta t^{-1}\left(F(t+\Delta t) - F(t)\right) + D\left[\theta_C F(t) + (1-\theta_C)F(t+\Delta t)\right] \\ & + \lambda(-1 + \varsigma^*)\left[\theta_J F(t) + (1-\theta_J)F(t+\Delta t)\right] \end{aligned}$$

where $\theta_C, \theta_J \in [0, 1]$ are constants. Rearranging yields

$$\begin{aligned} [1/\Delta t - \theta_C D - \theta_J\lambda(-1 + \varsigma^*)]F(t) \;=\; & [1/\Delta t + (1-\theta_C)D \\ & + (1-\theta_J)\lambda(-1 + \varsigma^*)]F(t+\Delta t). \quad (16) \end{aligned}$$

There are various ways of arranging (16) for numerical solution. The most obvious, corresponding to a standard Crank-Nicolson finite difference scheme, $\theta_C = \theta_J = 1/2$, is not practically feasible because after discretizing the x-space into N points inversion of a full $N \times N$ matrices is required, a computationally costly procedure of order N^3 per time step. Note that full matrix inversion has to be performed at every step since the parameters vary in both time and state. The state-dependent parameters also preclude use of Fourier transform techniques to solve the inversion problem. Explicit schemes, $\theta_C = \theta_J = 0$, are computationally feasible but potentially unstable and suffer from the drawback that their convergence in the time domain are only of $O(\Delta t)$, unlike Crank-Nicolson schemes that have precision of $O(\Delta t^2)$. When using FFT techniques to handle the convolution integral,

the computational order of the explicit scheme is $O(N \log_2 N)$ per time step. Schemes of the type $\theta_C = 1/2, \theta_J = 0$ are stable and efficient but accuracy is lost due to the asymmetric treatment of the continuous and jump part. Numerical experiments show that biases are introduced in the solution, particularly for long dated options.

In our experience, the best numerical solution method is an ADI (Alternating Directions Implicit) method where each time-step in the grid is split into two half-steps. For the first half-step we set $\theta_C = 1, \theta_J = 0$, which gives us

$$\left[\frac{1}{\Delta t/2} - D\right] F(t + \Delta t/2) = \left[\frac{1}{\Delta t/2} - \lambda + \lambda\varsigma^*\right] F(t + \Delta t). \tag{17a}$$

In a discrete grid this can be solved by first computing the convolution $\varsigma^* F(t + \Delta t)$ in discrete Fourier space, where

$$\langle\varsigma^* F(t + \Delta t)\rangle = \langle\varsigma\rangle\langle F(t + \Delta t)\rangle.$$

If we observe that $\langle\varsigma\rangle$ only needs to be computed once, the computational cost associated with the convolution part of (17a) is one FFT and one inverse FFT, i.e. $O(N \log_2 N)$. We further note that the discrete version of the differential operator D is a tri-diagonal matrix. Consequently, once the RHS of (17a) is obtained by FFT methods, then the system (17a) can be solved at a cost of $O(N)$. Hence, the total cost of solving (17a) is $O(N \log_2 N)$.

For the second half-step we set $\theta_C = 0, \theta_J = 1$, whereby

$$\left[\frac{1}{\Delta t/2} + \lambda - \lambda\varsigma^*\right] F(t) = \left[\frac{1}{\Delta t/2} + D\right] F(t + \Delta t/2). \tag{17b}$$

Letting $y = [2/\Delta t + D] F(t + \Delta t/2)$, now take the Fourier transform of (17b) to arrive at

$$(2/\Delta t + \lambda)\langle F(t)\rangle - \lambda\langle\varsigma\rangle\langle F(t)\rangle = \langle y\rangle \Rightarrow \langle F(t)\rangle = \langle y\rangle / (2/\Delta t + \lambda - \lambda\langle\varsigma\rangle). \tag{18}$$

We can now transform the equation back to obtain $F(t)$. All in all this requires one tri-diagonal matrix multiplication, one FFT and one inverse FFT, i.e. a procedure with a computational burden of $O(N \log_2 N)$.

To formally specify the discrete scheme described in (17a–b) we define the operators

$$\delta_x f(x) = \frac{1}{2\Delta x} \left[f(x + \Delta x) - f(x - \Delta x)\right],$$

$$\delta_{xx} f(x) = \frac{1}{(\Delta x)^2} \left[f(x + \Delta x) - 2f(x) + f(x - \Delta x)\right],$$

$$\bar{D} f(x) = \left[-r + a\delta_x + \tfrac{1}{2}b^2\delta_{xx}\right] f(x); \quad \bar{\varsigma}^* f(x) = \sum_j q_j(x) f(j\Delta x),$$

$$q_j(x) = \int_{(j-1/2)\Delta x}^{(j+1/2)\Delta x} \varsigma(x - y)\, dy.$$

We can then write the discrete version of (17a–b) as

$$\left[2/\Delta t - \bar{D}\right] F(t + \Delta t/2) = \left[2/\Delta t - \lambda + \lambda\bar{\varsigma}^*\right] F(t + \Delta t), \tag{19a}$$

$$\left[2/\Delta t + \lambda - \lambda\bar{\varsigma}^*\right] F(t) = \left[2/\Delta t + \bar{D}\right] F(t + \Delta t/2). \tag{19b}$$

The following proposition describes some important properties of the scheme (19a–b).

Proposition 3 *The following properties hold for the scheme (19a–b):*

(i) The scheme is unconditionally stable in the von Neumann sense.

(ii) For the case of deterministic parameters, the numerical solution of the scheme is locally accurate to order $O(\Delta t^2 + \Delta x^2)$.

(iii) If M is the number of time steps and N is the number of steps in the spatial direction, the computational burden is $O(MN \log_2 N)$.

Proof. (iii) was shown above. (i) and (ii) are shown in Appendix.

The presence of jumps increases the magnitude of the first-order derivative in the PDE relative to the no-jump case. This again can potentially cause oscillations for certain types of option payouts; see Zvan, Forsyth, and Vetzal (1998) for details. While we have not experienced any such difficulties, we point out that they can be remedied if necessary by evaluating first-order derivatives using an upwind scheme (Zvan, Forsyth, and Vetzal (1998)), at the cost of reducing the convergence order in the x-domain to $O(\Delta x)$.

3.2. Refinements

While the scheme described by (19a–b) is attractive in that it is unconditionally stable and only requires $O(N \log_2 N)$ operations per time step, a direct application suffers from certain drawbacks. Specifically, accurate representation of the convolution integral will generally require a very wide grid. Since the FFT algorithm only accepts uniform step length in the x-direction, the precision of the numerical solution in areas of interest might suffer. To overcome this, we here define an algorithm that assumes linearity of the option price outside a grid of size equal to a number of standard deviations of the underlying process. The linear part can conveniently be solved in closed-form[16] whereas the inner grid is solved using the FFT-ADI-algorithm described in (19a–b) above.

We split the function in two parts:[17]

$$F = F1_{x \in (\underline{x}, \bar{x})} + F1_{x \notin (\underline{x}, \bar{x})} \equiv G + H,$$

On $x \in (\underline{x}, \bar{x})$, G solves

$$0 = \frac{\partial G}{\partial t} + DG + \lambda(\varsigma^* - 1)F = \frac{\partial G}{\partial t} + DG - \lambda G + \lambda\varsigma^*[G + H].$$

If we assume that H is linear in e^x we can write

$$H(t, x) \cong \left[g_l(t)e^x + h_l(t)\right] 1_{x < \underline{x}} + \left[g_u(t)e^x + h_u(t)\right] 1_{x > \bar{x}},$$

where g_l, h_l, g_u, h_u are deterministic functions. This means that we can write

$$
\begin{aligned}
\varsigma^* H(t, x) \cong\ & g_l(t)e^x(1 + m(t)) \Pr'(x + \ln J(t) < \underline{x}) \\
& + h_l(t) \Pr(x + \ln J(l) < \underline{x}) \\
& + g_u(t)e^x(1 + m(l)) \Pr'(x + \ln J(l) > \bar{x}) \\
& + h_u(t) \Pr(x + \ln J(t) > \bar{x})
\end{aligned}
\tag{20}
$$

where $\Pr(\cdot)$ denotes probability under the distribution defined by ς and $\Pr'(\cdot)$ denotes probability under the distribution described by the Radon-Nikodym transformed density: $\varsigma'(t, x) = \varsigma(t, x)e^x/(1 + m(t))$. In the Merton (1976) case of log-normal jumps these probabilities can be computed in closed-form as Gaussian distribution functions. If the distribution of the jumps is non-parametric, the probabilities can be calculated by simple numerical integration over the densities ς, ς'.

We now get the following system

$$
\begin{aligned}
[2/\Delta t - D]G(t + \Delta t/2) &= (2/\Delta t - \lambda)G(t + \Delta t) + \lambda\varsigma^*G(t + \Delta t) \\
&\quad + \lambda\varsigma^*H(t + \Delta t) \\
&\quad, [2/\Delta t + \lambda - \lambda\varsigma^*]G(t) \\
&= [2/\Delta t + D]G(t + \Delta t/2) + \lambda\varsigma^*H(t),
\end{aligned}
\tag{21}
$$

where terms of the type ς^*G are handled numerically by FFTs and terms of the type ς^*H are handled by (20). The assumption of linearity of H amounts to stating that the functions g_l, g_u, h_l, h_u can be obtained from the asymptotes of a function defined by

$$
rf = f_t + (r(t) - q(t)) f_x
\tag{22}
$$

subject to the same boundary conditions as (13). Over a discrete time-step (22) has the closed-form solution

$$
f(t, x) = e^{-r\Delta t} f(t + \Delta t, x + (r(t) - q(t))\Delta t).
\tag{23}
$$

(23) together with the boundary conditions define g_l, g_u, h_l, h_u.

The scheme described above scheme can be used for most applications, including barrier options and options with Bermudan or American style exercise.

3.3. A Numerical Example

In this section we give a quick example of the practical performance of the method that has been outlined in the previous section. Table 3 below compares Merton's (1976) exact formula for European puts and calls (equation (8)) with the prices generated by the algorithm (19a–b), refined as discussed in the previous section. To stress the algorithm, the jump parameters have been set to fairly extreme values:

$$
r = 0.05, \quad q = 0.02, \quad \sigma = 0.15, \quad \lambda = 0.1, \quad \gamma = 0.4, \quad S(0) = 100, \quad K = 100
$$

The number of time steps is set to half the number of x-steps. Also, due to the usage of the FFT algorithm, the number of x-steps have been set to multiples of 2.

Table 3 also lists CPU times and the experimental convergence order of the method, the latter computed as the average slope of a log-log plot of absolute error against the time step. It is clear form the table that the convergence of the algorithm is smooth and approximately of order 2 in the number of time- and x-steps—a little higher for short-dated options and a little lower for long-dated options. This experimentally confirms the second statement of Proposition 3. In order to obtain accuracy to one basis point, Table 3 shows that generally 512 steps in the x-direction are necessary. CPU time for such a calculation is less than 1 second on a 400 MHz Pentium PC.

Table 3. Prices of European calls and puts using ADI-FFT PIDE solver.

	$T = 0.01, \mu = -1.08$		$T = 0.01, \mu = 0.92$		$T = 1, \mu = -1.08$		
x-steps	Put	Call	Put	Call	Put	Call	CPU Time
32	0.5330	0.5577	0.4324	0.4570	7.4882	10.3924	0.01
64	0.5512	0.5759	0.5612	0.5858	7.6711	10.5683	0.02
128	0.5552	0.5798	0.5929	0.6175	7.7101	10.6057	0.06
256	0.5561	0.5807	0.5995	0.6241	7.7193	10.6145	0.21
512	0.5563	0.5809	0.6011	0.6257	7.7216	10.6167	0.90
1024	0.5564	0.5810	0.6015	0.6261	7.7222	10.6172	6.88
Closed-form	0.5564	0.5810	0.6016	0.6262	7.7224	10.6174	0.00
Conv. Order	2.05	2.05	2.07	2.07	2.05	2.06	NA
	$T = 1, \mu = 0.92$		$T = 10, \mu = -1.08$		$T = 10, \mu = 0.92$		
x-steps	Put	Call	Put	Call	Put	Call	CPU Time
32	10.1666	12.9430	17.8984	39.9230	28.8594	41.4292	0.01
64	12.0254	14.8927	17.9780	39.4001	27.3118	46.3351	0.02
128	12.4263	15.3146	17.9972	39.2688	27.4585	48.1286	0.06
256	12.5051	15.3985	18.0018	39.2362	27.5255	48.6093	0.21
512	12.5239	15.4185	18.0030	39.2280	27.5420	48.7293	0.90
1024	12.5284	15.4234	18.0033	39.2260	27.5461	48.7593	6.88
Closed-form	12.5299	15.4250	18.0034	39.2253	27.5474	48.7693	0.00
Conv. Order	2.12	2.12	2.01	2.00	1.98	1.90	NA

Note: European put and call option prices of Merton model computed using FFT-ADI method with different number of state space steps on the main grid. The number of time steps is set to half the number of x- steps. CPU times are in seconds. The process parameters are $r = 0.05$, $q = 0.02$, $\sigma = 0.15$, $\lambda = 0.1$, $\gamma = 0.4$, $S(0) = 100.0$, $K = 100.0$.

3.4. *Monte Carlo Simulation*

The finite-difference method outlined in the previous sections is primarily useful for options with mild path-dependency (such as American options and barrier options), but is difficult to apply to options than depend more strongly on the path of the underlying stock. For such options, Monte Carlo simulation methods are generally useful (see Boyle *et al.* (1997) for a good review). Once the methods in Section 1 have been applied to determine the local volatility function, the SDE (1) can be simulated directly in an Euler scheme. For each time step one would determine whether there is a jump or not by randomizing over the jump probability ($\lambda \Delta t$) and then subsequently randomize over the jump distribution to determine the size of the jump. This procedure, however, is computationally inferior to other methods that explicitly exploit the independence of the jumps and the Brownian motion. One such procedure is described below.[18]

Let $\{\tau_j\}_{j=1,2,...}$ be the arrival times of the Poisson process π. We know that $\{\tau_{j+1} - \tau_j\}_{j=1,2,...}$ are mutually independent with distribution given by

$$\Pr(\tau_{j+1} - \tau_j > s) = \exp\left(-\int_{\tau_j}^{\tau_j+s} \lambda(u)\, du\right)$$

For each path we wish to simulate we use this to draw the arrival times for the particular

path up to our time horizon that we are considering. We then construct an increasing simulation time line that includes the jump times and our time horizon, say $\{t_i\}_{i=0,1,\ldots}$. The price process is now simulated as

$$
\begin{aligned}
S(t_i) &= F(0, t_i)e^{x(t_i)}, \\
x(t_i) &= -\int_0^{t_i} \lambda(u)m(u)\,du - \frac{1}{2}\sum_{k=0}^{i-1}\sigma(t_k, x(t_k))^2(t_{k+1} - t_k) \\
&\quad + \sum_{k=0}^{i-1}\sigma(t_k, x(t_k))\sqrt{t_{k+1} - t_k}\,\varepsilon(t_k) + \sum_{k=1}^{i} 1_{t_k \in \{\tau_j\}} \ln J(t_k)
\end{aligned}
\tag{24}
$$

and $\{\varepsilon(t_i)\}_{i=0,\ldots}$ is a sequence of independent standard normal random variables, and $\{J(\tau_j)\}_{j=1,2,\ldots}$ is a sequence of independent random variables drawn according to the marginal distributions $\{\varsigma(\tau_j; \cdot)\}_{j=1,2,\ldots}$.

The simulation scheme described by (24) is $O(\sqrt{\Delta t})$ convergent to the true stochastic differential equation and ensures that simulated stock prices have expectations equal to their forwards. Higher order accuracy simulation schemes can be constructed using the Taylor-expansion techniques described in Kloeden and Platen (1992).

4. Option Pricing: Numerical Tests

In this section we will combine the calibration results from Section 2 with the pricing algorithm of Section 3. First, we investigate what evolution of the volatility smile is implied in the model. Second, we price a range of standard option contracts. Throughout, we compare the results of the jump-diffusion model to the results of the DVF model. Both the DVF and jump-diffusion calibrations were tested for accuracy by numerically pricing all call options in the input set (Table 1); in all cases, the computed prices were within the bid-offer spreads.

4.1. Evolution of Volatility Skew

To illustrate the differences between the pure diffusion model and the jump-diffusion model, it is illuminating to investigate the volatility skews that the two models generate at future dates and stock price levels. In Table 4 we show the implied Black-Scholes volatilities for 1-year call options at different times and future levels of the underlying index in the jump-diffusion model.

Table 4 shows that the volatility skew of the jump-diffusion model is surprisingly stable over time and stock price levels. This is not the case for the fitted DVF model, as is obvious from Table 5 below. In particular, we notice that the future implied volatility skews of the fitted pure diffusion model are highly non-stationary and tend to flatten out as time progresses. In a few cases, the implied volatility surface even turns into a smile or otherwise becomes non-monotonic in the strike.

Table 4. Future 1-year S&P500 volatility skews in jump-diffusion model.

Strike (K), % of Future Spot (S)

	50	70	80	85	90	95	100	105	110	115	120	130	140	150	160	170	180	200
							S(t) = 70% of today's spot											
t = 0	47.35	36.64	31.23	28.83	26.75	25.02	23.54	22.18	20.91	19.87	19.29	19.57	19.97	19.75	19.41	19.14	18.89	19.27
t = 2	47.41	36.49	30.36	27.11	23.76	20.95	19.27	18.43	17.73	17.28	17.11	17.14	17.14	16.95	16.94	17.09	17.46	18.82
t = 4	47.35	36.60	31.28	29.19	27.68	26.56	25.45	24.49	23.77	23.15	22.58	21.55	20.39	19.46	18.90	18.64	18.68	19.50
t = 6	47.51	36.96	32.17	30.23	28.60	27.25	26.14	25.19	24.35	23.59	22.88	21.64	20.55	19.67	19.10	18.80	18.81	19.62
t = 8	47.69	37.19	32.50	30.52	28.80	27.44	26.44	25.59	24.77	24.01	23.28	22.00	21.01	20.20	19.59	19.19	19.08	19.73
							S(t) = 100% of today's spot											
t = 0	47.39	36.61	31.19	29.24	28.01	26.85	25.47	24.05	22.77	21.71	20.74	19.12	18.21	17.59	17.27	17.41	18.04	19.97
t = 2	47.23	36.55	30.99	28.54	26.40	24.46	22.68	21.22	20.16	19.36	18.72	17.83	17.39	17.21	17.21	17.38	17.82	19.13
t = 4	47.24	36.64	31.08	28.47	26.05	23.84	21.96	20.58	19.61	18.93	18.49	18.16	18.07	18.07	18.12	18.20	18.40	19.28
t = 6	47.36	36.64	31.06	28.41	25.97	23.82	22.02	20.65	19.65	18.96	18.52	18.19	18.24	18.32	18.46	18.67	18.97	19.84
t = 8	47.53	36.76	31.22	28.62	26.28	24.27	22.59	21.24	20.19	19.41	18.85	18.37	18.32	18.33	18.38	18.53	18.76	19.57
							S(t) = 130% of today's spot											
t = 0	47.20	36.52	30.67	27.77	25.04	22.56	20.52	19.05	17.96	17.10	16.48	16.05	16.73	18.09	19.46	20.56	21.42	22.59
t = 2	47.15	36.61	30.74	27.94	25.41	23.28	21.64	20.49	19.68	19.13	18.73	18.23	18.15	18.15	18.16	18.21	18.35	19.14
t = 4	47.37	36.54	30.76	28.15	25.95	24.29	23.09	22.18	21.46	20.94	20.53	19.82	19.36	19.05	18.85	18.78	18.84	19.48
t = 6	47.45	36.54	30.79	28.22	26.09	24.50	23.42	22.72	22.19	21.77	21.46	21.10	20.96	20.93	20.98	21.07	21.19	21.56
t = 8	47.54	36.63	30.91	28.31	26.12	24.47	23.37	22.62	22.03	21.54	21.16	20.67	20.37	20.19	20.08	20.05	20.08	20.40

Note. Future implied volatility skews in the jump-diffusion model fitted to S&P data. The reported implied Black-Scholes volatilities are for 1-year options. The first column reports the current time in years. For each of the three stock price levels, strikes are reported in percent of the stock price level.

Table 5. Future 1-year S&P500 volatility skews in the pure diffusion model.

										Strike (K), % of Future Spot (S)								
	50	70	80	85	90	95	100	105	110	115	120	130	140	150	160	170	180	200
								S(t) = 70% of today's spot										
t = 0	51.98	54.20	53.55	52.66	51.47	50.04	48.47	46.86	45.22	43.56	41.89	38.74	36.04	33.90	32.22	30.90	29.84	28.20
t = 2	44.01	44.68	42.83	41.66	40.48	39.40	38.42	37.48	36.56	35.67	34.85	33.35	32.05	30.96	30.04	29.25	28.57	27.48
t = 4	37.72	37.03	35.54	34.95	34.53	34.18	33.78	33.38	32.99	32.60	32.23	31.53	30.89	30.30	29.77	29.29	28.86	28.13
t = 6	34.81	33.50	32.76	32.66	32.51	32.31	32.10	31.88	31.66	31.45	31.24	30.82	30.42	30.04	29.69	29.36	29.07	28.54
t = 8	33.28	31.89	31.74	31.70	31.58	31.42	31.28	31.13	30.98	30.83	30.69	30.41	30.14	29.88	29.64	29.40	29.18	28.81
								S(t) = 100% of today's spot										
t = 0	47.67	36.74	31.32	28.95	26.94	25.30	24.01	23.01	22.24	21.64	21.17	20.51	20.70	19.78	19.60	19.52	19.53	19.94
t = 2	35.65	30.86	29.01	28.21	27.51	26.89	26.35	25.88	25.47	25.10	24.78	24.24	23.79	23.44	23.15	22.90	22.70	22.35
t = 4	31.89	30.29	29.30	28.84	28.41	28.02	27.65	27.32	27.01	26.73	26.47	26.02	25.63	25.29	25.01	24.79	24.57	24.14
t = 6	29.57	30.00	29.41	29.12	28.84	28.57	28.31	28.07	27.84	27.63	27.43	27.07	26.74	26.49	26.27	26.04	25.82	25.41
t = 8	29.32	29.89	29.48	29.27	29.07	28.87	28.68	28.50	28.32	28.16	28.01	27.74	27.50	27.30	27.09	26.88	26.68	26.30
								S(t) = 130% of today's spot										
t = 0	31.44	25.50	24.62	24.62	24.81	25.14	25.61	26.20	26.88	27.64	28.47	30.24	32.03	33.63	34.87	35.72	36.25	36.74
t = 2	25.36	24.89	23.95	23.57	23.25	22.98	22.73	22.52	22.34	22.17	22.04	21.79	21.60	21.42	21.24	21.07	20.91	20.65
t = 4	25.36	26.41	25.70	25.39	25.11	24.86	24.62	24.42	24.23	24.06	23.92	23.69	23.44	23.19	22.94	22.73	22.52	22.21
t = 6	24.87	27.27	26.76	26.52	26.29	26.09	25.89	25.72	25.56	25.44	25.32	25.06	24.79	24.53	24.28	24.06	23.88	23.58
t = 8	26.90	27.94	27.53	27.33	27.14	26.98	26.83	26.70	26.57	26.45	26.32	26.04	25.78	25.54	25.32	25.12	24.95	24.69

Note: Future implied volatility skews in the pure diffusion model (DVF) model fitted to S&P data. The reported implied Black-Scholes volatilities are for 1-year options. The first column reports the time in years. For each of the three stock price levels, strikes are reported in percent of the stock price level.

Table 6. S&P500 option prices: Jump-diffusion versus pure diffusion.

	Fwd starting call spread		Bermudan 80% put		Asian 120% call	
Option Maturity	Jump-Diffusion	Pure Diffusion (DVF)	Jump-Diffusion	Pure Diffusion (DVF)	Jump-Diffusion	Pure Diffusion (DVF)
1.0	8.79	8.73	3.06	3.02	0.46	0.46
2.0	7.68	7.40	5.40	5.07	2.18	2.12
3.0	7.28	6.79	7.22	6.61	4.35	4.19
4.0	6.87	6.32	8.70	7.90	6.50	6.26
5.0	6.49	5.88	9.93	8.96	8.50	8.22
6.0	6.09	5.51	10.94	9.78	10.30	10.00
7.0	5.73	5.15	11.76	10.43	11.92	11.62
8.0	5.43	4.85	12.45	10.97	13.40	13.11
9.0	5.16	4.59	13.05	11.42	14.71	14.43
10.0	4.91	4.35	13.55	11.81	15.88	15.63

Note: Exotic option prices (in % of current spot) for the jump-diffusion and DVF models. Both models are fitted to the S&P500 data in Section 2. The call spread prices refer to the prices of forward starting 100-120 strike 1-year call option spreads, i.e. the prices in 4th row and 2nd and 3rd columns of the table is today's percentage price of an option that pays $(S(4)/S(3) - 100\%)^+ - (S(4)/S(3) - 120\%)^+$ at year 4. The Bermudan option prices are the prices of put options with a strike of 80% of initial spot, with the right to exercise once every month. The Asian call prices refer to the prices of 120% strike call options on the arithmetic monthly average. Forward starting and Asian option prices were computed from 100,000 simulations. The simulation standard error is everywhere less than 1% of the option price. The Bermudan option prices were computed using the FFT-ADI method on a grid of size 128×256.

4.2. *Prices of Exotic Options*

The different evolution of the implied volatility skew in the jump-diffusion and DVF models obviously will have consequences for the pricing of exotic options that, unlike European puts and calls, depend on the full dynamics of the stock price, rather than just the distribution at a single point in time. Options that fall in this category include compound options and barrier options, but also most near-"vanilla" contracts, including American/Bermudan options, forward starting options, and Asian options. Table 6 below report the prices of some of these contracts in the jump-diffusion and DVF models fitted to the S&P500 data in Section 2.

It is obvious from the results in Table 6 that the jump-diffusion and DVF models return significantly different prices for Bermudan and forward starting options, and that this difference grows as the maturity is increased. The differences in the Asian option prices are smaller but still significant.

5. Conclusion

This paper has presented a framework for adding Poisson jumps to the standard DVF (Deterministic Volatility Function) diffusion models of stock price evolution. We have developed a forward PIDE (Partial Integro-Differential Equation) for the evolution of call option prices as functions of strike and maturity, and shown how this equation can be used

in an efficient calibration to market quoted option prices. To employ the calibrated model to pricing of various exotic options, we have developed an efficient ADI (Alternating Direction Implicit) finite-difference technique with attractive stability and convergence properties.

Applying our calibration algorithm to the S&P500 market results in a largely constant diffusion volatility overlaid with a significant jump component. For the S&P500 market, we find diffusion volatilities around 15–20% and, working in the risk-neutral probability measure, a 9% (annual) chance of an index drop averaging around 50%. In light of the current internet stock debacle, it is possible that the market objectively assigns such high probabilities of large crashes, but the fairly extreme values of the risk-neutral jump parameters more likely reflects risk premia relative to historical parameters. Indeed, a general equlibrium analysis reveals that the historical jump process implied by the risk-neutral jump parameters is quite reasonable. In any case, numerically fitting a jump-diffusion model to the S&P500 market is both easier and more robust than fitting a DVF model: lacking the jump component to handle the significant short-term skew in S&P500 volatilities, the latter model requires very steep and highly time-dependent local volatilities to match market prices.

As the paper demonstrates, the evolution of the volatility smile in a DVF model fitted to S&P500 data is highly non-stationary and often counterintuitive. The jump-diffusion model, on the other hand, produces almost perfect stationary S&P500 volatility skews. Despite giving virtually identical prices for European options, the two models differ significantly in their pricing of a range of standard exotic option contracts.

While this paper has mainly focused on equities, we point out that the developed methodology works equally well for FX rates. As most FX markets exhibit volatility smiles, rather than skews, calibration to such market will typically result in less directional jump processes, with the mean jump being closer to 0 than is the case for stocks.

6. Appendix

Proof of Proposition 1. Consider a twice differentiable function $H(S(t))$. With stock price dynamics as in (1), the evolution of $H(S(t))$ is given by the *Doleans-Dade-Meyer extension* to Ito's lemma (see e.g. Krishnan (1984), p. 184):

$$
\begin{aligned}
dH(S(t)) \;=\; & H_S(S(t-))(r(t) - q(t) - \lambda(t)m(t))S(t-)dt \\
& + \tfrac{1}{2}H_{SS}(S(t-))\sigma(t, S(t-))^2 S(t-)^2 dt \\
& + H_s(S(t-))\sigma(t, S(t-))S(t-)dW(t) \\
& + [H(J(t)S(t-)) - H(S(t-))]\, d\pi(t) \tag{A.1}
\end{aligned}
$$

Now, set $H(S(t)) = (S(t) - K)^+$ for a fixed positive number K. While this function is not differentiable in the usual sense, let us nevertheless proceed formally as in (A.1):

$$
\begin{aligned}
d(S(t) - K)^+ \;=\; & 1_{S(t-)>K}(r(t) - q(t) - \lambda(t)m(t))S(t-)dt \\
& + \tfrac{1}{2}\delta(S(t-) - K)\sigma(t, K)^2 K^2 dt \\
& + 1_{S(t-)>K}\sigma(t, S(t-))S(t-)dW(t) \\
& + \big[(J(t)S(t-) - K)^+ - (S(t-) - K)^+\big]\, d\pi(t) \tag{A.2}
\end{aligned}
$$

where 1_A denotes the indicator function for the set A and $\delta(\cdot)$ is Dirac's delta function. (A.2) can, in fact, be justified rigorously by the *Tanaka-Meyer formula* (see Karatzas and Shreve (1991), p. 218) and is equivalent to the integral representation

$$
\begin{aligned}
(S(T) - K)^+ = {} & (S(t) - K)^+ + \int_t^T 1_{S(v-)>K}(r(v) - q(v) - \lambda(v)m(v))S(v-)\,dv \\
& + \int_t^T \tfrac{1}{2}\delta(S(v-) - K)\sigma(v, K)^2 K^2\,dv \\
& + \int_t^T 1_{S(v-)>K}\sigma(v, S(v-))S(v-)\,dW(v) \\
& + \int_t^T \left[(J(v)S(v-) - K)^+ - (S(v-) - K)^+\right]d\pi(v). \qquad \text{(A.3)}
\end{aligned}
$$

In (A.3), the term $\tfrac{1}{2}\int_t^T \delta(S(v-) - K)\sigma(v, K)^2 K^2\,dv$ is normally called the *local time at K* over the time interval $[t, T]$.

By standard pricing theory, the time t price of a T-maturity European call option struck at K is

$$
C(t, S(t); T, K) = e^{-\int_t^T r(v)\,dv} E_t\left[(S(T) - K)^+\right], \qquad \text{(A.4)}
$$

where, as before, $E_t[\cdot]$ denotes risk-neutral expectation conditional on the information revealed up to time t. Assuming sufficient regularity for an application of Fubini's theorem (interchange of time integration and expectation), (A.3) and (A.4) yield

$$
\begin{aligned}
C(t, S(t); T, K)e^{\int_t^T r(v)\,dv} = {} & (S(t) - K)^+ + \\
& \int_t^T (r(v) - q(v) \\
& - \lambda(v)m(v)E_t\left[1_{S(v)>K}S(v)\right]dv \\
& + \int_t^T \tfrac{1}{2}E_t\left[\delta(S(v) - K)\right]\sigma(v, K)^2 K^2\,dv \\
& + \int_t^T E_t\left[(J(v)S(v) - K)^+ - (S(v) - K)^+\right]\lambda(v)\,dv, \quad \text{(A.5)}
\end{aligned}
$$

where we have used the martingale property of the stochastic integral over $W(t)$; the fact that $S(t)$ and $S(t-)$ are identically distributed; and the independence of W, J, and π.

In (A.5) the expectation of the Dirac delta function equals the stock price density, and hence, from a standard result in Breeden and Litzenberger (1978),

$$
E_t\left[\delta(S(v) - K)\right] = e^{\int_t^v r(u)\,du} C_{KK}(t, S(t); v, K).
$$

Moreover, it is easily verified that

$$
\begin{aligned}
C(t, S(t); v, K)e^{\int_t^v r(u)\,du} = {} & E_t\left[1_{S(v)>K}(S(v) - K)\right] \\
= {} & E_t\left[1_{S(v)>K}S(v)\right] + Ke^{\int_t^v r(u)\,du}C_K(t, S(t); v, K).
\end{aligned}
$$

Inserting these results into (A.5) and differentiating with respect to T yields

$$
\begin{aligned}
C_T(t, S(t); T, K) \;=\; & (-q(T) - \lambda(T)m(T))C(t, S(t); T, K) \\
& + \tfrac{1}{2}\sigma(T, K)^2 K^2 C_{KK}(t, S(t); T, K) \\
& - (r(T) - q(T) - \lambda(T)m(T))K C_K(t, S(t); T, K) \\
& + \lambda(T)e^{-\int_t^T r(u)\,du} E_t\left[(J(T)S(T) - K)^+\right] \\
& - \lambda(T)e^{-\int_t^T r(u)\,du} E_t\left[(S(T) - K)^+\right].
\end{aligned}
\tag{A.6}
$$

By the independence assumption and (A.4),

$$
\begin{aligned}
e^{-\int_t^T r(u)\,du} E_t\left[(J(T)S(T) - K)^+\right] &= e^{-\int_t^T r(u)\,du} E_t\left[J(T)\,(S(T) - K/J(T))^+\right] \\
&= \int_{-\infty}^{\infty} z C\left(t, S(t); T, K/z\right) \zeta(z; T)\,dz \\
&= (1 + m(T))\int_0^{\infty} C\left(t, S(t); T, K/z\right) \zeta'(z; T)\,dz.
\end{aligned}
$$

where $\zeta'(z; T) \equiv z\zeta(z; T)/(1 + m(T))$ is a probability density function as $J(T) > 0$ (a.s.), $1 + m(T) > 0$, and $E\left[J(T)/(1 + m(T))\right] = 1$.

The above identity together with another application of (A.4) reduces (A.6) to the result in Proposition 1.

Proof of Proposition 3. We first consider the von Neumann stability. Inserting $u_1(t, x) = \vartheta_1^{-t}e^{ikx}$ into (19a) and $u_2(t, x) = \vartheta_2^{-t}e^{ikx}$ and (19b), where ϑ_1, ϑ_2 are complex numbers, yields

$$
\begin{aligned}
\vartheta \equiv \vartheta_1^{\Delta t/2} \cdot \vartheta_2^{\Delta t/2} \;=\; & \frac{\left[2/\Delta t + (-r + a\delta_x + \tfrac{1}{2}b^2\delta_{xx})\right]e^{ikx}}{\left[2/\Delta t - (-r + a\delta_x + \tfrac{1}{2}b^2\delta_{xx})\right]e^{ikx}} \\[2mm]
& \cdot \frac{2e^{ikx}/\Delta t - \lambda e^{ikx} + \lambda \sum_j q_j(x)e^{ikj\Delta x}}{2e^{ikx}/\Delta t + \lambda e^{ikx} - \lambda \sum_j q_j(x)e^{ikj\Delta x}}
\end{aligned}
$$

The von Neumann criterion (Mitchell and Griffiths (1980), p. 38) for stability requires that $|\vartheta| \leq 1$ for all integers k. Straightforward calculations show that $\vartheta = A(k) \cdot B(k)$, where

$$
A(k) = \frac{\frac{2}{\Delta t} - r - \frac{b^2}{\Delta x^2}(1 - \cos k\Delta x) + i\frac{a}{\Delta x}\sin k\Delta x}{\frac{2}{\Delta t} + r + \frac{b^2}{\Delta x^2}(1 - \cos k\Delta x) - i\frac{a}{\Delta x}\sin k\Delta x},
$$

$$
B(k) = \frac{2/\Delta t - \lambda\left(1 - \sum_j q_j(x)\cos kj\Delta x\right) + i\lambda\sum_j q_j(x)\sin kj\Delta x}{2/\Delta t + \lambda\left(1 - \sum_j q_j(x)\cos kj\Delta x\right) - i\lambda\sum_j q_j(x)\sin kj\Delta x}.
$$

A geometric argument shows that $|A(k)| \leq 1$ when $r \geq 0$ for all k. Noting that

$$
\sum_j q_j(x)\cos kj\Delta x \leq \sum_j q_j(x) = 1,
$$

another geometric argument demonstrates that also $|B(k)| \leq 1$ for all k. In total, we conclude that the scheme is *unconditionally stable*.

Turning to the issue of precision, we first note that

$$F(s) = \left[\sum_{n=0}^{\infty} \frac{(s-t)^n}{n!} \left(\frac{\partial}{\partial t} \right)^n \right] F(t) = e^{(s-t)\frac{\partial}{\partial t}} F(t).$$

At the same time we have that

$$0 = \left[\frac{\partial}{\partial t} + D + \lambda(\varsigma^* - 1) \right] F$$

These two properties together with the fact that, in the case of deterministic parameters, the operators D and ς^* commute imply that we can write

$$e^{-\frac{\Delta t}{2}D} F(t + \Delta t/2) = e^{\frac{\Delta t}{2}\lambda(\varsigma^*-1)} F(t + \Delta t), \ e^{\frac{\Delta t}{2}\lambda(\varsigma^*-1)} F(t) = e^{\frac{\Delta t}{2}D} F(t + \Delta t/2).$$

Expanding the exponentials yields

$$\left[1 - \tfrac{1}{2}\Delta t D + \tfrac{1}{2}(\Delta t/2)^2 D^2 \right] F(t + \Delta t/2) =$$
$$\left[1 + \tfrac{1}{2}\Delta t \lambda(\varsigma^* - 1) \right.$$
$$\left. + \tfrac{1}{2}(\Delta t/2)^2 \lambda^2(\varsigma^* - 1)^2 \right] F(t + \Delta t) + O(\Delta t^3),$$
$$\left[1 - \tfrac{1}{2}\Delta t \lambda(\varsigma^* - 1) + \tfrac{1}{2}(\Delta t/2)^2 \lambda^2(\varsigma^* - 1)^2 \right] F(t)$$
$$= \left[1 + \tfrac{1}{2}\Delta t D + \tfrac{1}{2}(\Delta t/2)^2 D^2 \right] F(t + \Delta t/2) + O(\Delta t^3).$$

We now note that for arbitrary analytic functions f, we have that

$$\overline{D} f(x) = D f(x) + O(\Delta x^2), \ \overline{\varsigma}^* f(x) = \varsigma^* f(x) + O(\Delta x^2).$$

Inserting this gives us the two equations

$$\left[1 - \tfrac{1}{2}\Delta t \overline{D} \right] F(t + \Delta t/2) = \left[1 + \tfrac{1}{2}\Delta t \lambda(\overline{\varsigma}^* - 1) \right] F(t + \Delta t)$$
$$+ \tfrac{1}{2}(\tfrac{1}{2}\Delta t)^2 \left(-\overline{D}^2 F(t + \Delta t/2) + \lambda^2(\overline{\varsigma}^* - 1)^2 F(t + \Delta t) \right) + O(\Delta t \Delta x^2 + \Delta t^3),$$
$$\left[1 - \tfrac{1}{2}\Delta t \lambda(\overline{\varsigma}^* - 1) \right] F(t) = \left[1 + \tfrac{1}{2}\Delta t \overline{D} \right] F(t + \Delta t/2)$$
$$+ \tfrac{1}{2}(\tfrac{1}{2}\Delta t)^2 \left(\overline{D}^2 F(t + \Delta t/2) - \lambda^2(\overline{\varsigma}^* - 1)^2 F(t) \right) + O(\Delta t \Delta x^2 + \Delta t^3).$$

Substituting the first equation into the second equation yields

$$\left[1 - \tfrac{1}{2}\Delta t \lambda(\overline{\varsigma}^* - 1) \right] F(t) = \left[1 + \tfrac{1}{2}\Delta t \overline{D} \right] \left[1 - \tfrac{1}{2}\Delta t \overline{D} \right]^{-1}$$
$$\times \left[1 + \tfrac{1}{2}\Delta t \lambda(\overline{\varsigma}^* - 1) \right] F(t + \Delta t)$$
$$+ \left[1 + \tfrac{1}{2}\Delta t \overline{D} \right] \left[1 - \tfrac{1}{2}\Delta t \overline{D} \right]^{-1} \tfrac{1}{2}(\tfrac{1}{2}\Delta t)^2 \left(-\overline{D}^2 F(t + \Delta t/2) + \right.$$
$$\left. \lambda^2(\overline{\varsigma}^* - 1)^2 F(t + \Delta t) \right)$$
$$+ \tfrac{1}{2}(\tfrac{1}{2}\Delta t)^2 \left(\overline{D}^2 F(t + \Delta t/2) - \lambda^2(\overline{\varsigma}^* - 1)^2 F(t) \right) + O(\Delta t \Delta x^2 + \Delta t^3)$$

where the term $[1 - \tfrac{1}{2}\Delta t \overline{D}]^{-1}$ should be interpreted in the sense of matrix inversion. We

now use the two observations

$$\left[1 - \tfrac{1}{2}\Delta t \overline{D}\right]^{-1} = 1 + O(\Delta t); \; F(t + \Delta t) = F(t) + O(\Delta t)$$

to conclude that

$$\left[1 - \tfrac{1}{2}\Delta t \lambda(\overline{\varsigma}^* - 1)\right] F(t) = \left[1 + \tfrac{1}{2}\Delta t \overline{D}\right]\left[1 - \tfrac{1}{2}\Delta t \overline{D}\right]^{-1}\left[1 + \tfrac{1}{2}\Delta t \lambda(\overline{\varsigma}^* - 1)\right]$$
$$\times F(t + \Delta t) + O(\Delta t \Delta x^2 + \Delta t^3) \qquad \text{(A.7)}$$

(A.7) is just another way of writing (19a–b). Hence, we can conclude that the local truncation error of the scheme (19a–b) is $O(\Delta t \Delta x^2 + \Delta t^3)$, and thereby that the local accuracy of the scheme is of order $O(\Delta t^2 + \Delta x^2)$.

Notes

1. The degree of incompleteness is higher in a jump-diffusion model than in a stochastic volatility model. Whereas stochastic volatility models can be made complete by the introduction of one (or a few) traded options, a jump-diffusion model typically requires the existence of a continuum of options for the market to be complete.
2. As discussed in Section 1, the risk-neutral measure is not necessarily unique for jump-diffusions of the type (1). If the measure is not unique, i.e. we work in an incomplete market with only a finite set of options traded on S, (1) should be interpreted as being valid for some explicit choice of measure. By fitting the parameters of (1) to market prices, this choice of measure effectively becomes the market measure.
3. Note that integration over the Poisson differential $d\pi$ is to be interpreted as a Stieltjes integral (see for instance Krishnan (1984), p. 155).
4. The payoff of a European call option at maturity is $C(T, S; T, K) = (S - K)^+$.
5. In particular, we would just replace $\sigma^2(T, K)$ with $E_t\left[\sigma^2(T) \mid S(T) = K\right]$.
6. We thank George Skiadopoulos for making us aware of Luca Pappalardo's working paper.
7. We notice that (6) is not invertible (in the sense that $\sigma^2(\cdot) \geq 0$ exists) for arbitrary choices of the constant jump parameters.
8. On a philosophical note, we point out that this assumption effectively leads to a complete market: the jump component can be hedged by taking a position in a continuum of call options with equal maturity and with strikes spanning the interval $[0, \infty[$. In practice, this type of "hedge" is, of course, not realistic.
9. Typically the norm minimized is a weighted sum of the least-squares aggregate price error and a regularity term measuring the smoothness of the local volatility function.
10. Surprisingly, many papers (including most of the ones cited here) suboptimally use the backward PDE to compute the prices of the call options to which the model is fitted. In effect, each iteration in the search algorithm involves solving one PDE per option in the target set (rather than just a single PDE, which would be the case if the forward equation was used).
11. For a quick derivation of this result, see Andreasen and Gruenewald (1996).
12. As discussed in Footnote 7, (9) will not have a meaningful solution $\hat{s}$ for arbitrary choices of the jump parameters. Clearly, we would require that the chosen parameters satisfy $M(t, T, k, 0) < (\Psi t; T, k)$ for all relevant T and k.
13. If this is not the case, we can either extend the grid or evaluate the contributions to the integral outside the range of ω by extrapolation methods.
14. In the sense of minimizing the RMS of relative errors on the risk-neutral parameters λ and μ.
15. For the standard backward PIDE (2) we have $x = \ln S, a = r - q - \lambda m - \tfrac{1}{2}\sigma^2, b = \sigma$.
16. This technique of approximating the option value outside the main grid as a linear function and computing it in closed-form was also used in Andreasen (1998).

17. Here 1_A denotes the indicator function on the set A.

18. If the jump intensity is constant, one can also a) first draw the *number* of jumps for a particular path by sampling the Poisson distribution directly; and then b) simulate the *location* on the time-line of these jumps. Step b) is simple as jump-times are uniformly distributed on the simulation horizon when conditioned on the number of jumps.

References

Ait-Sahalia, Y., Yubo Wang, and Francis Yared. (1998). "Do Option Markets Correctly Asses the Probabilities of Movements of the Underlying Asset?" Forthcoming, *Journal of Econometrics*.

Amin, Kaushuk. (1996). "Jump Diffusion Option Valuation in Discrete Time," *Journal of Finance* 48, 1833–1863.

Andersen, Leif, and Rupert Brotherton-Ratcliffe. (1998). "The Equity Option Volatility Smile: A Finite Difference Approach," *Journal of Computational Finance* 1, 2, 5–38.

Andersen, Torben, Luca Benzoni, and Jesper Lund. (1999). "Estimating Jump-Diffusions for Equity Returns," Working Paper, Northwestern University and Aarhus School of Business.

Andreasen, Jesper. (1997). "Implied Modelling: Stable Implementation, Hedging, and Duality," Working Paper, University of Aarhus.

Andreasen, Jesper. (1998). "The Pricing of Discretely Sampled Asian and Lookback Options: A Change of Numeraire Approach," *Journal of Computational Finance* 2, 1, 5–30.

Andreasen, Jesper, and Barbara Gruenewald. (1996). "American Option Pricing in the Jump-Diffusion Model," Working Paper, Aarhus University and University of Mainz.

Avallaneda Marco, Craig Friedman, Richard Holmes, and Dominick Samperi. (1997). "Calibrating Volatility Surfaces via Relative-Entropy Minimization," *Applied Mathematical Finance* 4, 1.

Bakshi, Gurdip, Charles Cao, and Zhiwu Chen. (1997). "Empirical Performance of Alternative Option Pricing Models," *Journal of Finance* 52, 2003–2049.

Bates, David. (1996). "Jumps and Stochastic Volatility: Exchange Rate Processes Implicit in Deutsche Mark Options," *Review of Financial Studies* 9, 1, 69–107.

Bjork, Tomas, Yuri Kabanov, and Wolfgang Runggaldier. (1997). "Bond Market Structure in the Presence of Marked Point Processes," *Mathematical Finance* 7, 211–239.

Black, Fischer, and Myron Scholes. (1973). "The Pricing of Options and Corporate Liabilities," *Journal of Political Economy* 81, 637–654.

Boyle, Phelim, Mark Broadie, and Paul Glasserman. (1997). "Monte Carlo Methods for Security Pricing," *Journal of Economic Dynamics and Control* 21, 8–9, 1267–1321.

Breeden, Douglas, and Robert Litzenberger. (1978). "Prices of State-Contingent Claims Implicit in Options Prices," *Journal of Business* 51, October, 621–651.

Brown, Gregory, and Klaus Toft. (1999). "Constructing Implied Binomial Trees from Multiple Probability Distributions," *Journal of Derivatives* 7, 2, 83–100.

Buraschi, Andrea, and Jens Jackwerth. (1998). "Explaining Option Prices: Deterministic vs. Stochastic Models," Working Paper, London Business School.

Coleman, Thomas, Yuying Li, and Arun Verma. (1999). "Reconstructing the Optimal Volatility Surface," *Journal of Computational Finance* 2, 3, 77–102.

Chriss, Neill. (1996). "Transatlantic Trees," *RISK* July, 45–48.

Das, Sanjiv, and Silverio Foresi. (1996). "Exact Solutions for Bond and Option Prices with Systematic Jump Risk," *Review of Derivatives Research* 1, 7–24.

Derman, Emanuel and Iraj Kani. (1994). "Riding on a Smile," *RISK Magazine* February, 32–39.

Dierckx, Paul. (1995). *Curve and Surface Fitting with Splines*. Oxford Science Publications.

Dumas, Bernard, Jeff Fleming, and Robert E. Whaley. (1997). "Implied Volatility Functions: Empirical Tests," *Journal of Finance* 53, 2059–2106.

Duffie, Darrell, Jun Pan, and Kenneth Singleton. (1999). "Transform Analysis and Option Pricing for Affine Jump-Diffusions," Working Paper, Stanford University.

Dupire, Bruno. (1994). "Pricing with a Smile," *RISK Magazine* January, 18–20.

Heston, Steven. (1993). "A Closed-Form Solution for Options with Stochastic Volatility with Applications to Bond and Currency Options," *Review of Financial Studies* 6, 2, 327–343.

Hull, John, and Allan White. (1987). "The Pricing of Options with Stochastic Volatilities," *Journal of Finance* 42, 281–300.

Jackwerth, Jens. (1996). "Generalized Binomial Trees," Working Paper, University of California at Berkeley.

Karatzas, Ioannis, and Steven Shreve. (1991). *Brownian Motion and Stochastic Calculus*. Springer Verlag.

Kloeden, Peter, and Eckhardt Platen. (1992). *Numerical Solution of Stochastic Differential Equations*. Springer Verlag.

Krishnan, Venkatarama. (1984). *Nonlinear Filtering and Smoothing*. John Wiley and Sons.

Lagnado, Ronald, and Stanley Osher. (1997). "Reconciling Differences," *RISK Magazine* April, 79–83.

Merton, Robert. (1976). "Option Pricing when Underlying Stock Returns are Discontinuous," *Journal of Financial Economics* May, 125–144.

Mitchell, Andrew, and D. F. Griffiths. (1980). *The Finite Difference Method in Partial Differential Equations*. John Wiley & Sons.

Naik, Vasant, and Moon Lee. (1990). "General Equilibrium Pricing of Options on the Market Portfolio with Discontinuous Returns," *The Review of Financial Studies* 3, 493–521.

Papparlardo, Luca. (1996), "Option Pricing and Smile Effect when Underlying Stock Prices are Driven by a Jump Process," Working Paper, University of Warwick.

Press, William H., Saul A. Teukolsky, William T. Vetterling and Brian P. Flannery. (1992). *Numerical Recipes in C*. Cambridge University Press.

Rubinstein, Mark. (1994). "Implied Binomial Trees," *Journal of Finance* 49, 771–818.

Stein, Elias, and Jeremy Stein. (1991). "Stock Price Distributions with Stochastic Volatility: An Analytic Approach," *Review of Financial Studies* 4, 4, 727–752.

Zhang, X. (1993). "Options Americaines et Modeles de Diffusion avec Sauts," *C. R. Acad. Sci. Paris*, Serie I, 857–862.

Zvan, Robert, Peter Forsyth, and Kenneth Vetzal. (1998). "Robust Numerical Methods for PDE Models of Asian Options," *Journal of Computational Finance* 1, 39–78.